DOI: 10.1002/cssc.201402428

Redox-Initiated Hydrogel System for Detection and Real-Time Imaging of Cellulolytic Enzyme Activity

Klara H. Malinowska, Tobias Verdorfer, Aylin Meinhold, Lukas F. Milles, Victor Funk, Hermann E. Gaub, and Michael A. Nash*[a]

Understanding the process of biomass degradation by cellulolytic enzymes is of urgent importance for biofuel and chemical production. Optimizing pretreatment conditions and improving enzyme formulations both require assays to quantify saccharification products on solid substrates. Typically, such assays are performed using freely diffusing fluorophores or dyes that measure reducing polysaccharide chain ends. These methods have thus far not allowed spatial localization of hydrolysis activity to specific substrate locations with identifiable morphological features. Here we describe a hydrogel reagent signaling (HyReS) system that amplifies saccharification products and initiates crosslinking of a hydrogel that localizes to locations of cellulose hydrolysis, allowing for imaging of the degradation process in real time. Optical detection of the gel in a rapid parallel format on synthetic and natural pretreated solid substrates was used to quantify activity of *T. emersonii* and *T. reesei* enzyme cocktails. When combined with total internal reflection fluorescence microscopy and AFM imaging, the reagent system provided a means to visualize enzyme activity in real-time with high spatial resolution (<2 μm). These results demonstrate the versatility of the HyReS system in detecting cellulolytic enzyme activity and suggest new opportunities in real-time chemical imaging of biomass depolymerization.

Introduction

Multistep bioconversion processes for production of liquid fuels and other chemical commodities from biomass are poised to alter our energy future. One step on the route to biomass-derived fuels is the enzymatic hydrolysis of cellulosic materials into fermentable sugars, a keystone in the overall process. Cellulolytic enzymes are used in large quantities to depolymerize cellulose chains into energy-dense glucose monomers and other short chain cellodextrins prior to fermentation.[1] In order to achieve high conversion rates in practice, enzymatic saccharification requires high enzyme loadings (e.g., 20 mg enzyme $g_{substrate}^{-1}$) and can be costly and inefficient.[2] To make the process more efficient and affordable, pretreatment methods that render the substrate more susceptible to enzymatic degradation have been developed.[3] Additionally, enzyme cocktails secreted from the aerobic fungus *Trichoderma reesei* (*Tr*) are being steadily improved to exhibit synergism among components for industrial processes.[4] This continued improvement has meanwhile drawn attention to a major challenge in the field, namely that of assaying and quantifying the effectiveness of cellulolytic enzyme formulations on a range of substrates possessing variable composition, morphology, degrees of crystallinity, and/or lignin content.

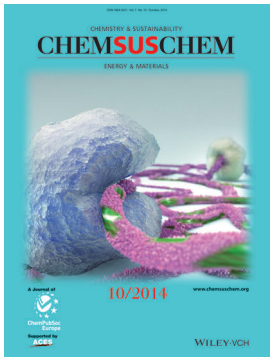

COVER

In the past, cellulase assays have been performed using a suite of bulk biochemical methods.[5–13] These include a variety of assays which measure the content of reducing polysaccharide chain ends using redox-sensitive absorbing dyes [e.g., 3,5-dinitrosalicylic acid (DNS)]. Other methods include the glucose oxidase (GOx)/horseradish peroxidase system (HRP)[14] which provides a fluorescent readout, or HPLC combined with quantitative mass spectrometry,[15] which reports on the quantity and size distribution of hydrolyzed chains. Electrochemical biosensors have also been employed to detect cellulase activity.[16]

More recently, methods for observing the spatial localization of cellulolytic activity have garnered interest as well. Imaging substrate locations susceptible to enzymatic hydrolysis could allow correlation of digestibility with substrate features such as fiber bundle size, degree of fiber branching, and/or crystal orientation. Conventional high-resolution imaging methods (e.g., TEM, SEM) are performed under vacuum and therefore are not suitable for monitoring enzymatic digestibility under biocompatible conditions. AFM imaging in liquid has shown promise, and has been used to observe disintegration of ultraflat micro-

[a] K. H. Malinowska,[+] T. Verdorfer,[+] A. Meinhold, L. F. Milles, V. Funk, Prof. Dr. H. E. Gaub, Dr. M. A. Nash
Lehrstuhl für Angewandte Physik and Center for Nanoscience
Ludwig-Maximilians-Universität
Amalienstrasse 54, 80799 Munich (Germany)
E-mail: michael.nash@lmu.de

[+] These authors contributed equally to this work.

Supporting Information for this article is available on the WWW under http://dx.doi.org/10.1002/cssc.201402428.

tomed substrates.[17,18] Time-resolution using AFM imaging is limited by scan times of up to several minutes and substrates are limited to ultraflat artificial cellulose surfaces (i.e., no native fibrils). Stimulated Raman spectroscopy has also been shown to provide adequate spatial and temporal resolution[19] and can be used on natural biomass substrates, however it is technically involved, requiring synchronization of multiple lasers at different wavelengths with modulation in the MHz range. Single-molecule fluorescence has shown potential for providing insights into cellulolytic enzyme function, but, so far, studies have only focused on carbohydrate binding modules and their cooperativity,[20–22] and the method has not been used to directly detect cellulolytic enzyme activity. Typically, soluble fluorescent enzyme substrates will diffuse away too quickly to allow for localization of activity. A fluorescent reagent system that could be used to directly read hydrolysis activity in an imaging modality could provide new insights to enzymatic activity and synergy.

Since its discovery in the late 19th century, hydroxyl radicals produced via Fenton chemistry have found use in many industrial applications, ranging from removal of organics from contaminated wastewater,[23] to redox-initiated free radical polymerization.[24,25] More recently in the biomaterials field, Fe^{II} Fenton reagents have been combined with GOx to achieve spatially controlled release of hydroxyl radicals from pre-existent poly(ethylene glycol) (PEG) hydrogels. For example, spatial confinement of radical generation at an interface was used to prepare multilayer particles.[26] Fluorescent gels could also be produced in response to immuno-recognition events.[27–29]

Here we extend the use of Fe^{II} Fenton reagents, and demonstrate their application in a cellulase-mediated polymerization system capable of monitoring cellulose hydrolysis in real time. The hydrogel reagent signaling system (HyReS system) described here detects cellulolytic enzyme activity with good sensitivity and is compatible with a variety of readout formats, including bulk turbidity and fluorescence as well as spatially-resolved total internal reflection fluorescence (TIRF) and AFM imaging, as depicted in Figure 1 d. The HyReS system relies on an Fe^{II} Fenton reagent that is oxidized by hydrogen peroxide with concomitant production of a reactive hydroxyl radical.

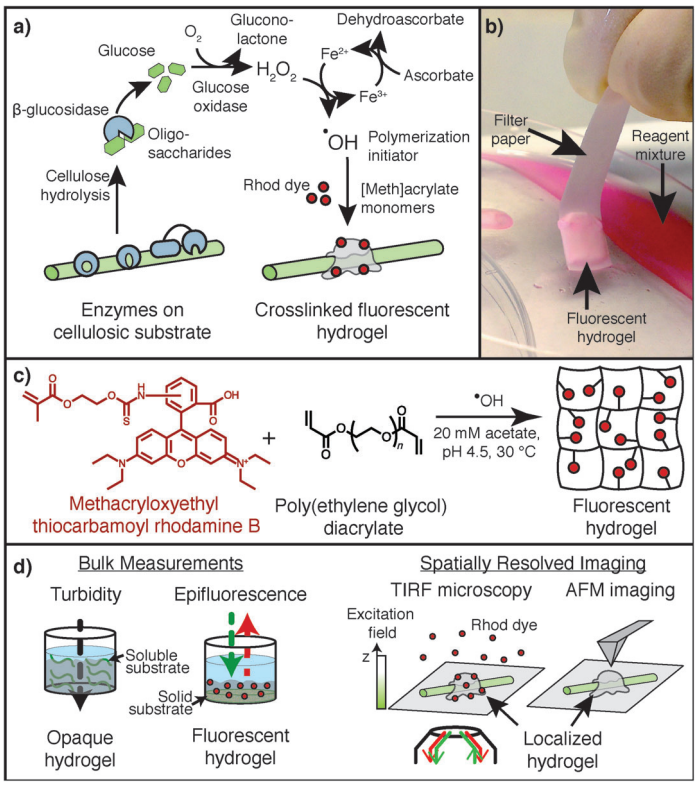

Figure 1. Overview of hydrogel reagent signaling (HyReS) system for detecting and imaging the degradation of cellulosic substrates. a) Saccharification products are converted into H_2O_2 via reaction with β-glucosidase and GOx. H_2O_2 proceeds with an Fe^{2+}-Fenton reagent to produce hydroxyl radicals that initiate hydrogel crosslinking. b) Photograph of filter paper partially submerged in the HyReS mixture for 30 min. c) Scheme showing structures of Rhod dye and gel cross-linker PEG diacrylate. d) Detection of the hydrogel using bulk measurements and spatially resolved imaging. Left: Bulk measurements in a parallel 96-well format provide a method for screening substrate pretreatment conditions or optimizing enzyme formulations on soluble and solid substrates. Right: High-resolution imaging methods such as TIRF microscopy and AFM-imaging allow detection of gel formation locally on fiber surfaces.

Results and Discussion

An overview of the HyReS system is shown in Figure 1 a. We used enzyme formulations that incorporated the synergistic endo- and exoglucanase activities of cellulolytic enzymes together with the cellobiase activity of β-glucosidase. β-glucosidase is frequently supplemented into cellulolytic enzyme formulations to convert cellobiose to glucose, thereby removing a primary inhibitor of exoglucanases in the cocktail.[30] In our system, β-glucosidase is responsible for production of glucose, which is further oxidized by GOx, directly producing H_2O_2, a reactant in the Fenton reaction. Gel formation proceeded via hydroxyl radical initiated polymerization of PEG diacrylate in the mixture, as depicted in Figure 1 c. Figure 1 b shows a representative gel film that polymerized onto a piece of filter paper upon partial submersion into the HyReS system containing 1 mg mL^{-1} *Tr* enzyme cocktail for 30 min. The composition of the HyReS mixture can be found in Table 1.

Table 1. Composition of the HyReS system.

Component	Concentration
glucose oxidase	1 mg mL^{-1}
$FeSO_4$	250 μM
ascorbic acid	250 μM
PEG diacrylate (M_n 575)	15 wt%
acetate buffer, pH 4.5	20 mM
rhodamine B methacrylate	3.5 μM (epifluorescence)/35 nM (TIRF)/ none (turbidity, AFM)
cellulolytic enzymes	0–2 mg mL^{-1}

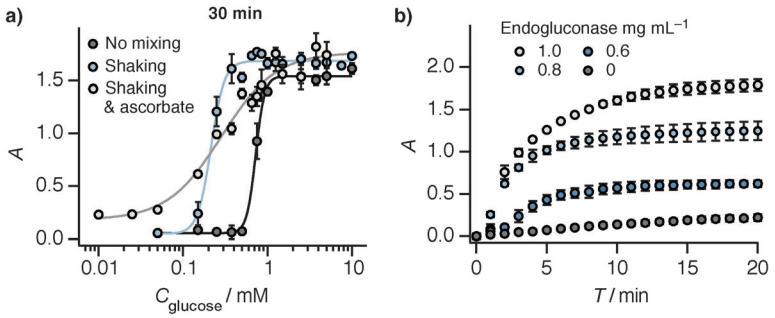

Figure 2. Detection of hydrogel polymerization by turbidity measurements on soluble substrates. a) Glucose standards were added to the HyReS system in a 96-well plate format. Absorbance at 600 nm due to light scattering by the polymerized hydrogel was measured after 30 min. Fits were performed using the Hill equation. b) Varying amounts of endoglucanase were added to CMC and the HyReS system. Turbidity was monitored over time. Gel polymerization proceeded proportional to CMCase activity of the enzyme and could be followed continuously in real time.

Initially, we tested the sensitivity of the HyReS system in detecting glucose directly added to sample wells of a 96-well plate. Since the PEG hydrogel turned the solution turbid as it polymerized, the absorbance signal at 550 nm increased with the amount of glucose in the solution. The results from a glucose standard curve measured after 30 min reaction time are shown in Figure 2a. A glucose detection limit in the low micromolar range was found. This sensitivity is similar to that found for microtiter plate DNS assays[31] and is generally sufficient for assaying cellulases involved in biomass conversion. Improvement in sensitivity was achieved by rotary shaking of the plate during the reaction. Inclusion of ascorbic acid in a 1:1 molar ratio with $FeSO_4$ also improved the sensitivity by serving as a weak reducing agent in the HyReS system, reducing Fe^{III} back to Fe^{II}, thereby regenerating the Fenton catalyst in situ.[32] When using the standard HyReS system (Table 1) for detecting glucose, the dynamic range of detection was from 0.05 to 5 mM (Figure 2a).

Figure 2b shows an endoglucanase assay performed on the soluble cellulose analog carboxymethyl cellulose (CMC). Varying amounts of β-1,4-endoglucanase from the thermophilic fungus *Talaromyces emersonii* were added to 30 mM solutions of CMC and the HyReS system at 37 °C (without ascorbic acid in this case). Turbidity increased with CMCase activity in a concentration dependent manner. Interestingly, the final absorbance values achieved by different endoglucanase concentrations were not the same, suggesting the kinetics of polymerization affect the final absorbance signal generated. This result was likely attributable to differences in gel density which led to different optical extinction properties, or alternatively due to entrapment of the endoglucanase during hydrogel polymerization that restricted access to the CMC substrate.

Although CMC is commonly used for screening endoglucanase activity, it is a poor predictor of hydrolysis performance on pretreated natural biomass in the context of biofuel production. For this purpose, solid substrates are typically more informative. To demonstrate the capabilities of the HyReS system on relevant solid substrates, hydrolysis on a variety of solid substrates was measured using fluorescence detection. Initially, Whatman #1 filter paper (FP) was used as the source of glucose. FP was cut into 6 mm disks and placed into the wells of a 96-well plate. The HyReS system including a fluorescent rhodamine monomer (Rhod) was added to the FP disks, along with 1 mg mL^{-1} of *Tr* enzymes. At given time points, the wells were washed to remove unreacted dye molecules, and the fluorescence was measured (Figure 3A). The result after 120 min was a pink-colored gel that conformally coated the filter paper, observable by eye with macroscopic dimensions (several mm thick). When the reagent system was added in the absence of the hydrolytic enzymes, background fluorescence remained low, indicating

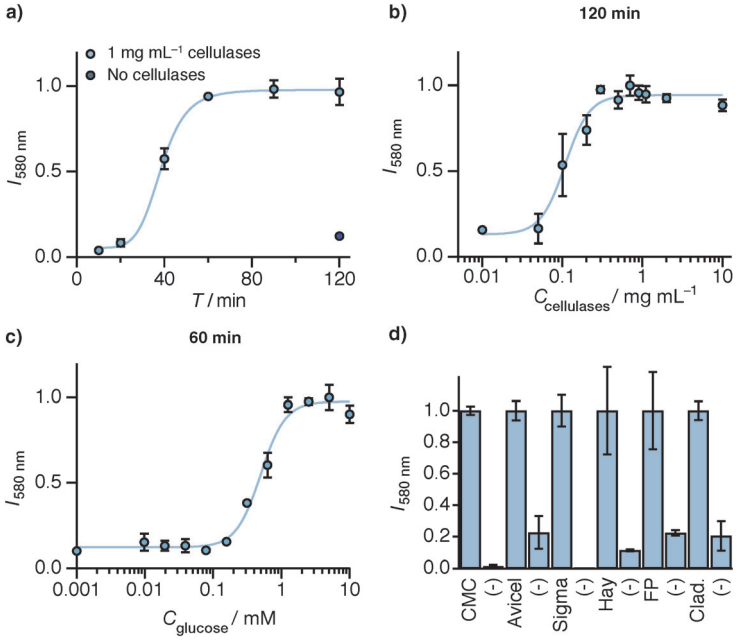

Figure 3. Detection of polymerization by Rhod fluorescence on solid substrates. a) Rhod fluorescence intensity vs. time for HyReS system/*Tr* enzyme cocktail on filter paper. Samples were rinsed and fluorescence signal read at given time points (dark blue circle, lacking *Tr* enzymes). Hill equation fits serve as a guide for the eye. b) Fluorescence intensity vs. *Tr* enzyme concentration measured on filter paper after 120 min. c) Glucose standard for solid substrate. Small volumes of glucose standards were applied onto the filter paper to ensure similar diffusion geometry as during enzymatic hydrolysis of the substrate. HyReS system without cellulases was applied and fluorescence intensity was measured after 60 min. d) HyReS system/*Tr* enzymes were applied to cellulosic substrates for 2 h. Normalized signal was robust in comparison with negative controls. CMC: carboxymethyl cellulose; Avicel: μ-crystalline cellulose; Sigma: μ-crystalline cellulose powder; Hay: dilute acid pretreated hay; FP: filter paper; Clad.: pretreated algal *Cladophora* cellulose.

that the hydrogel assay was specific. Figure 3b shows the fluorescence signal after 120 min exposure of the HyReS system with varying concentration of *Tr* cellulases to the filter paper. These data show that our detection method discriminates between different levels of cellulolytic activity, with a linear dynamic range for *Tr* enzyme cocktails from 0.05 to 0.3 mg mL^{-1}. The assay precision ranged from 2.0% at 0.3 mg mL^{-1} *Tr* enzymes to 52% at 0.05 mg mL^{-1} *Tr* enzymes.

To assay the absolute amount of glucose produced by cellulolytic enzymes on FP and not only the relative changes in activity, we calibrated the assay to glucose standards. To mimic the geometry of sugar release, FP disks were soaked with small volumes of concentrated glucose solutions in varying concentrations. The HyReS system including Rhod but lacking *Tr* enzymes was then added and samples were incubated for 1 h. Following rinsing, the fluorescence was measured (Figure 3c). The dynamic range of this standardization assay on glucose was found to be from 0.1 to 2 mM. We attribute the decrease of the sensitivity in comparison with turbidity assay to nonspecific binding of Rhod to FP. The decreased sensitivity in the high concentration range can be attributed to the readout method. While the turbidity assay intrinsically integrates the signal from full volume of hydrogel, fluorescence signal might only be read from a limited volume close to the gel surface, also dependent on gel density. Once this critical optical thickness of the gel is exceeded, the same signal will be measured for varying hydrogel coating thicknesses.

A small amount of nonspecific binding of Rhod to the solid substrates was observable, but in general was not problematic. Nonspecific binding is likely to be dependent on the type of substrate, its charge properties, and pretreatment conditions. Therefore, the performance of the HyReS system on a range of cellulose substrates was tested to determine its substrate compatibility profile. As shown in Figure 3c, the HyReS system with fluorescence detection was found to provide high signal-to-noise ratios on every substrate tested, including CMC, Avicel, Sigma μ-crystalline cellulose powder, dilute acid pretreated hay, filter paper, and pretreated algal *Cladophora* cellulose. Non-specific binding was not found to be a limitation, as indicated by the negative controls lacking the cellulolytic enzymes. The selectivity ratios of specific to non-specific signal ranged from 4.4 for Avicel to 751.9 for Sigma μ-crystalline cellulose powder. All results were statistically significant using a one-sided t-test to $P < 0.025$. The system therefore has a wide applicability and seems to provide high signal-to-noise ratios on nearly any cellulose substrate susceptible to enzymatic degradation.

The pH-dependence of the assay was investigated by preparing the HyReS system at various pH values from 4.5 to 7.5 (see the Supporting Information). A pH of 5.0 or below was necessary for the reaction due to base catalyzed oxidation of Fe^{II} to Fe^{III} at higher pH values and consequent quenching of the reaction.[33] This low pH requirement might be limiting for this system for some applications as fungal cellulases have pH optima in the range of 4 to 6.5.[34] However, the HyReS system pH range (< pH 5) matches optimal conditions for many cellulolytic enzyme formulations (e.g., *Tr* and *A. niger* cocktails).[35,36]

Developing systems for real-time imaging of cellulose degradation is an important step towards improved enzyme formulations for biofuel development. In order to facilitate real-time imaging we used TIRF microscopy, which only samples molecules within an evanescent field extending away from the glass surface to a distance of a few hundred nanometers. This method restricts the excitation volume in a similar manner to confocal microscopy.[37] We were able to use nM quantities of the Rhod dye while simultaneously rejecting the fluorescent background and imaging the buildup of gel on the cellulose fibers. This setup eliminated the need to rinse away any unreacted Rhod before readout, significantly improving time resolution. The refractive index of the hydrogel is less than that of glass, therefore the critical angle requirement for TIRF was maintained and excitation light did not penetrate into the bulk even as the gel formed at the surface.

Figure 4 shows time-lapse TIRF imaging with the HyReS system. *Cladophora* cellulose was covalently labeled with a fluorescein derivative[38] (5-(4,6-dichlorotriazinyl) aminofluorescein, DTAF), and patterned in lines onto a cover slip (see Experimental Section). The sample was then imaged under liquid in the TIRF microscope. Under blue illumination (See "TIRF-cellulose", Figure 4a and e), patterned bands of labeled cellulose fibers were clearly visible at the top and bottom of the image, and reproduced the fibrous structure of the *Cladophora* cellulose in the TIRF image. The cellulose-free band forms the black stripe in the center of the image. Next, *Tr* enzymes and HyReS system including Rhod dye at 35 nM were added to the liquid, and images were collected over time under green illumination (Figure 4b–d). At time $t = 0$, the gel had not yet formed and no Rhod signal was observable in the TIRF image (Figure 4B). By time $t = 60$ min., HyReS polymerization had incorporated Rhod into the hydrogel and the signal became observable in the TIRF image, mainly at locations where the cellulose was deposited, reproducing the substrate pattern with high fidelity (Figure 4d). This result indicated that reaction of the oligosaccharide hydrolysis products with the HyReS system components and initiation of polymerization occurred quickly enough to be localized to their site of production before the components could diffuse away from the fiber surface. Negative control experiments lacking the *Tr* enzyme mixtures (Figure 4e–h) showed only low non-specific signal that did not co-localize with the patterned substrate locations. The HyReS system therefore served as an imaging method and provided a fluorescent readout that increased from a low background to a high signal directly in response to hydrolysis of the substrate. To the best of our knowledge, such a localized chemical imaging system for cellulolytic activity has never been shown before using fluorescence detection. Such a method could provide distinct advantages in studies on cellulase synergy and susceptibility of cellulose substrates to degradation at specific locations (e.g., branch points, fibril ends, and/or crystalline faces).

To obtain more detailed information about the morphology of the hydrogel formation on solid substrates, we employed time resolved AFM imaging. DTAF-labeled cellulose was spin-coated uniformly onto a coverslip and the HyReS system was

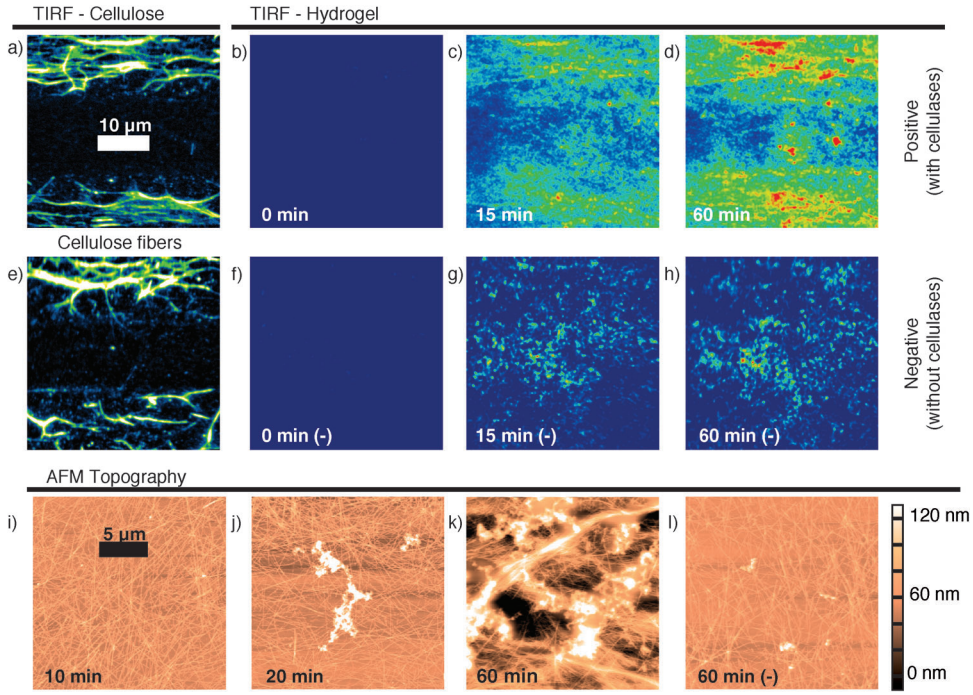

Figure 4. Time-lapse TIRF(a–h) and AFM (i–l) imaging. Cellulose fibers were covalently labelled with a fluorescein derivative (DTAF) and patterned onto a cover slip. The stripes of patterned cellulose were clearly visible in blue TIRF illumination, while a middle band of the cover slip remained cellulose-free (a and e). The HyReS mixture including 35 nM Rhod and 2 mg mL^{-1} *Tr* cellulases was added and sample was imaged under green illumination for 60 min (b, c, and d). Polymerization of the fluorescent hydrogel clearly co-localized with locations of micropatterned cellulose. The negative control experiment lacking *Tr* enzymes (images f, g, and h) showed only low nonspecific background that did not co-localize with substrate locations. AFM height images (i–l) were obtained on cellulose that was deposited uniformly across the entire cover glass and exposed to the HyReS mixture. Panel (l) shows the negative control (60 min (−)) lacking *Tr* enzymes.

applied for varying amounts of time. Afterwards, samples were carefully rinsed and imaged in tapping mode in air (Figure 4i–l). The Cladophora celluose formed a dense mat on the glass surface, consisting mostly of thin and long features corresponding to single cellulose fibers or small fiber bundles (Figure 4i). After 20 min, the HyReS system formed distinctive hydrogel features on the surface with heights of up to several hundred nm. The number and size of the features clearly increased with assay time. After an hour, large piles of hydrogel with heights of up to hundreds of nm and widths of several μm could be observed. This demonstrates the high signal amplification achieved by HyReS system because each hydroxyl radical initiates chain propagation that incorporates several hundred monomers into the growing gel. Additionally, the signal is integrated over time as the gel builds up. These amplification and integration mechanisms convert the glucose signal generated upon hydrolysis of nanometer-scale cellulose fibers into micrometer-scale hydrogel formations. At the same time, the size of the hydrogel formations originating from small cellulose features sets the intrinsic limit to the spatial resolution of presented method. The negative control showed small amounts of unspecific polymerization, consistent with our observations from TIRF imaging.

Conclusion

We have shown that the HyReS system, comprising a mixture of cellulolytic enzymes, β-glucosidase, GOx, Fe^{II}, ascorbic acid, PEG diacrylate, and Rhod is a versatile tool for detecting and imaging cellulolytic enzyme activity on a wide range of solid and soluble cellulose substrates. The system is compatible with turbidity detection on soluble substrates, and with fluorescence detection for insoluble substrates. Using the turbidity method, we have demonstrated glucose sensitivity in the low micromolar range which is on par with other bulk glucose determinations (e.g., DNS[31]). Analagous to conventional GOx/HRP systems, our system includes an amplification step as many vinylated monomers are incorporated into the growing gel for every hydroxyl radical initiator produced from glucose. Additionally, our system has other added advantages, such as localization of the signal to crystalline solid–liquid interfaces, and integration of the signal over time and space. We have furthermore presented results that demonstrate the HyReS system as an imaging platform for use in combination with TIRF microscopy and AFM, providing real-time imaging of cellulose hydrolysis with high spatial resolution. Our AFM imaging results demonstrate the extent of signal amplification that is possible when attempting to observe cellulose digestibility on nanometer-scale fibers. These unique features of the HyReS system can contribute to our understanding of how substrate structure affects enzymatic hydrolysis, and also move toward assaying the activity of individual cellulolytic complexes (i.e., cellulosomes) deposited onto cellulosic substrates. These results taken together establish the HyReS system as a competitive cellulase assay platform with the added advantage of spatially resolved localized chemical imaging.

Experimental Section

Materials: Methacryloxyethyl thiocarbamoyl rhodamine B (Rhod) was obtained from Polysciences Inc. (Warrington, PA, USA). Beta-1,4-endoglucanase from *T. emersonii* was purchased from Megazyme (Ireland). Glucose oxidase from *A. niger* and β-glucosidase from almonds were purchased from Sigma–Aldrich. All other reagents were obtained from Sigma–Aldrich and used without further purification. Composition of the standard reagent mixture

used for cellulase activity detection is shown in Table 1. All experiments used this standard mixture with slight variations noted in the text. Reagents were premixed prior to each experiment. Poly(propylene) 96-well were purchased from Grenier (Bio-One).

Turbidity measurements on soluble substrates: For the glucose calibration plot (Figure 2a), wells of a 96-well plate were filled with 100 μL of acetate buffer containing twice the target concentration of the HyReS system (Table 1). An equal volume of acetate buffer (100 μL) containing twice the target glucose concentration was added. Monitoring of the absorbance (600 nm) began immediately and continued for 30 min inside a plate reader (Tecan M1000 Pro) at 37 °C. The endoglucanase assay (Figure 2b) was performed similarly, using CMC in place of glucose. CMC (degree of substitution: 0.60–0.95) was dissolved in acetate buffer, pH 4.5. Each well was filled with a total volume of 100 μL containing the indicated amount of CMC, cellulolytic enzymes, and the standard HyReS reagent mixture (without Rhod dye). The plate was incubated at 37 °C inside a plate reader and absorbance was measured continuously at 550 nm. The reported errors correspond to the standard deviation of at least three independent measurements.

Fluorescence measurements on solid substrates: Filter paper (Whatman #1, FP) was cut into disks (6 mm diameter, 2.5 mg cellulose), placed into the wells of a 96-well plate and used as the cellulose substrate. For calibration of the assay, 5 μL of glucose standards were allowed to soak into the FP disks, followed by addition of 195 μL of HyReS system (lacking cellulases). After incubation at 37 °C, unreacted monomer was removed with a water rinse using a microplate strip washer (ELx50, BioTek). Fluorescence at 580 nm was measured in a plate reader with excitation at 555 nm. For the cellulase assays, a total liquid volume of 200 μL containing cellulolytic enzymes (range 0–1 mg mL^{-1}) together with 3.5 μM Rhod and the standard reagent mixture (Table 1) was added to each well. After incubation at 37 °C, polymerization was stopped by removing unreacted monomer with a water rinse using ELx50 Microplate Strip Washer (BioTech). Fluorescence was measured immediately with a plate reader (M1000pro, Tecan) with excitation at 555 nm, and emission at 580 nm. The reported errors correspond to the standard deviation of at least three independent measurements.

DTAF-grafted cellulose fibers (DTAF-CF): Cellulose fibers were extracted from fresh *Cladophora* algae according to published protocols.[39,40] Noncellulosic cell components were first extracted in 98% ethanol at 50 °C for 24 h. Solid material was filtered and subsequently boiled for 2 h in 0.1 M NaOH. After exchanging the NaOH solution, cellulose was again extracted at 80 °C overnight. Afterwards, the sample was immersed in 0.05 M HCl at room temperature for 12 h, filtered, thoroughly washed with water and freeze-dried. In order to obtain cellulose microcrystals, the sample was further acid hydrolyzed in 40% H_2SO_4 at 70 °C for 12 h. After extensive centrifugal separation and washing, cellulose was dialyzed against deionized water and the suspension was stored in water at 4 °C in darkness for up to several weeks prior to use.
Cladophora cellulose fibers obtained in this way were covalently labeled with the fluorescent dye DTAF according to previously published protocols.[38,42] In short, 5 mg of DTAF was dissolved in 1 mL of 0.2 M NaOH. The resulting solution was mixed with 500 μL of the cellulose suspension in water and reacted for 24 h at room temperature. Unreacted dye was removed by centrifugal washing five times followed by dialysis against water.

Cellulose micropatterning: Round cover slips (borosilicate, 22 mm dia., 0.2 mm thickness, Thermo Fisher) were aminosilanized following previously published procedures.[41] DTAF-labeled cellulose fibers were patterned on aminosilanized cover slips under flow in a PDMS microfluidic channel. A PDMS mold with two parallel channels 100 μm wide, 28 μm high and 2 cm long, spaced 15 μm apart was produced using standard soft lithography methods, and applied onto an aminosilanized glass surface and cured at 65 °C overnight. A suspension of DTAF-CF was sonicated for 3 min to disperse fibrils, introduced into the channels and incubated for 5 min. The negatively charged DTAF-CFs adhered to positively charged aminosilanized glass surface. Afterwards, the channels were flushed with water to remove weakly bound fibers. The flow channel was then removed, and surfaces were blocked for 2 h by exposure to a solution of 2 mg mL^{-1} BSA in acetate buffer (20 mM, pH 4.5) followed by rinsing with water.

Total internal reflection fluorescence microscopy: Fluorescence imaging was carried out in TIRF excitation on a custom-built multicolor TIRF microscope, similar to the instrument described previously by Gumpp et al.[43] Blue DTAF dye was excited by the 488 nm line and Rhod by the 561 nm line of the TOPTICA iChrome MLE-LFA laser through a 100×, NA 1.49 oil immersion objective lens (Nikon Apochromat). We used ET525/36 and HC600/37 emission filters mounted in Optosplit III (Carin Research) for detection of DTAF and Rhod fluorescence, respectively. The emitted light was detected using a 1024×1024 pixel back-illuminated EMCCD camera (Andor iXon3 888).
The cover glass with micropatterned lines of DTAF-CFs was placed in a liquid-tight holder and mounted on the fluorescence microscope. First, cellulose fibers in buffer were imaged under buffer to verify patterning fidelity. To visualize hydrogel build-up in real time, 300 μL of the standard reagent mixture supplemented with 2 mg mL^{-1} *Tr* cellulolytic enzymes, and 35 nM Rhod were added onto the sample. Time series were recorded in blue and green channels with an integration time of 0.5 s per frame and 10 s between acquisitions. The Peltier-cooled CCD chip was typically operated at a temperature of −80 °C and an electron multiplication gain of 150× and 200× was used for blue and green channels respectively.

Atomic force microscopy: Measurements were carried out using MFP-3D AFM (Asylum Research) in combination with AC160 cantilevers (resonance frequency: 300 kHz, spring constant: 27 N m^{-1}, Olympus). All imaging studies were done in tapping mode with amplitude of ~100 nm. DTAF-CFs were spin coated onto an aminosilanized cover slip (3000 rpm, 60 s). The standard hydrogel reagent mix including 1 mg mL^{-1} *Tr* cellulases was added to the cover slip and sample was incubated for varying amounts of time at 37 °C. Polymerization was stopped by a gentle rinse in a beaker of ultrapure water. The sample was blow dried with gentle nitrogen stream and imaged in air.

Acknowledgements

The authors gratefully acknowledge funding from the European Research Council and the Nanosystems Initiative Munich. M.A.N. acknowledges funding from Society in Science–The Branco Weiss Fellowship administered by the Swiss Federal Institute of Technology (ETH Zürich).

Keywords: biomass · cellulase enzymes · radical reactions · TIRF imaging · *Trichoderma reesei*

[1] M. E. Himmel, S.-Y. Ding, D. K. Johnson, W. S. Adney, M. R. Nimlos, J. W. Brady, T. D. Foust, *Science* **2007**, *315*, 804 – 807.
[2] D. Klein-Marcuschamer, P. Oleskowicz-Popiel, B. A. Simmons, H. W. Blanch, *Biotechnol. Bioeng.* **2012**, *109*, 1083 – 1087.
[3] P. Kumar, D. M. Barrett, M. J. Delwiche, P. Stroeve, *Ind. Eng. Chem. Res.* **2009**, *48*, 3713 – 3729.
[4] R. Peterson, H. Nevalainen, *Microbiology* **2012**, *158*, 58 – 68.
[5] W. Helbert, H. Chanzy, T. L. Husum, M. Schülein, S. Ernst, *Biomacromolecules* **2003**, *4*, 481 – 487.
[6] Y. H. P. Zhang, J. Hong, X. Ye in *Methods in Molecular Biology*, Humana Press, Totowa, NJ, **2009**, pp. 213 – 231.
[7] A. Chandrasekaran, R. Bharadwaj, J. I. Park, R. Sapra, P. D. Adams, A. K. Singh, *J. Proteome Res.* **2010**, *9*, 5677 – 5683.
[8] M. Dashtban, M. Maki, K. T. Leung, C. Mao, W. Qin, *Crit. Rev. Biotechnol.* **2010**, *30*, 302 – 309.
[9] D. R. Ivanen, N. L. Rongjina, S. M. Shishlyannikov, G. I. Litviakova, L. S. Isaeva-Ivanova, K. A. Shabalin, A. A. Kulminskaya, *J. Microbiol. Methods* **2009**, *76*, 295 – 300.
[10] D. J. Coleman, M. J. Studler, J. J. Naleway, *Anal. Biochem.* **2007**, *371*, 146 – 153.
[11] Y. H. Percival Zhang, M. E. Himmel, J. R. Mielenz, *Biotechnol. Adv.* **2006**, *24*, 452 – 481.
[12] Z. Xiao, R. Storms, A. Tsang, *Biotechnol. Bioeng.* **2004**, *88*, 832 – 837.
[13] R. Mullings, *Enzyme Microb. Technol.* **1985**, *7*, 586 – 591.
[14] S. Kongruang, M. K. Bothwell, J. McGuire, M. Zhou, R. P. Haugland, *Enzyme Microb. Technol.* **2003**, *32*, 539 – 545.
[15] V. Harjunpää, J. Helin, A. Koivula, M. Siika-aho, T. Drakenberg, *FEBS Lett.* **1999**, *443*, 149 – 153.
[16] N. Cruys-Bagger, S. F. Badino, R. Tokin, M. Gontsarik, S. Fathalinejad, K. Jensen, M. D. Toscano, T. H. Sørensen, K. Borch, H. Tatsumi, P. Väljamäe, *Enzyme Microb. Technol.* **2014**, *58 – 59*, 68 – 74.
[17] P. Bubner, J. Dohr, H. Plank, C. Mayrhofer, B. Nidetzky, *J. Biol. Chem.* **2012**, *287*, 2759 – 2765.
[18] T. Ganner, P. Bubner, M. Eibinger, C. Mayrhofer, H. Plank, B. Nidetzky, *J. Biol. Chem.* **2012**, *287*, 43215 – 43222.
[19] B. G. Saar, Y. Zeng, C. W. Freudiger, Y.-S. Liu, M. E. Himmel, X. S. Xie, S.-Y. Ding, *Angew. Chem. Int. Ed.* **2010**, *49*, 5476 – 5479; *Angew. Chem.* **2010**, *122*, 5608 – 5611.
[20] J. M. Fox, P. Jess, R. B. Jambusaria, G. M. Moo, J. Liphardt, D. S. Clark, H. W. Blanch, *Nat. Chem. Biol.* **2013**, *9*, 356 – 361.
[21] S. Y. Ding, Y. S. Liu, Y. Zeng, M. E. Himmel, J. O. Baker, E. A. Bayer, *Science* **2012**, *338*, 1055 – 1060.
[22] D. J. Dagel, Y.-S. Liu, L. Zhong, Y. Luo, M. E. Himmel, Q. Xu, Y. Zeng, S.-Y. Ding, S. Smith, *J. Phys. Chem. B* **2011**, *115*, 635 – 641.
[23] E. Neyens, J. Baeyens, *J. Hazard. Mater.* **2003**, *98*, 33 – 50.
[24] F. S. Dainton, P. H. Seaman, *J. Polym. Sci.* **1959**, *39*, 279 – 297.
[25] A. S. Sarac, *Prog. Polym. Sci.* **1999**, *24*, 1149 – 1204.
[26] R. Shenoy, M. W. Tibbitt, K. S. Anseth, C. N. Bowman, *Chem. Mater.* **2013**, *25*, 761 – 767.
[27] L. M. Johnson, C. A. DeForest, A. Pendurti, K. S. Anseth, C. N. Bowman, *ACS Appl. Mater. Interfaces* **2010**, *2*, 1963 – 1972.
[28] B. J. Berron, L. M. Johnson, X. Ba, J. D. McCall, N. J. Alvey, K. S. Anseth, C. N. Bowman, *Biotechnol. Bioeng.* **2011**, *108*, 1521 – 1528.
[29] H. D. Sikes, R. R. Hansen, L. M. Johnson, R. Jenison, J. W. Birks, K. L. Rowlen, C. N. Bowman, *Nat. Mater.* **2008**, *7*, 52 – 56.
[30] G. Gefen, M. Anbar, E. Morag, R. Lamed, E. A. Bayer, *Proc. Natl. Acad. Sci. USA* **2012**, *109*, 10298 – 10303.
[31] C. Gonçalves, R. M. Rodriguez-Jasso, N. Gomes, J. A. Teixeira, I. Belo, *Anal. Methods* **2010**, *2*, 2046.
[32] B. Halliwell, J. Gutteridge, *FEBS Lett.* **1992**, *307*, 108 – 112.
[33] T. Tabakova, D. Andreeva, A. Andreev, C. Vladov, I. Mitov, *J. Mater. Sci. Mater. Electron.* **1992**, *3*, 201 – 205.
[34] L. N. Anderson, D. E. Culley, B. A. Hofstad, L. M. Chauvigne-Hines, E. M. Zink, S. O. Purvine, R. D. Smith, S. J. Callister, J. M. Magnuson, A. T. Wright, *Mol. Biosyst.* **2013**, *9*, 2992 – 3000.
[35] T. Wang, X. Liu, Q. Yu, X. Zhang, Y. Qu, P. Gao, T. Wang, *Biomol. Eng.* **2005**, *22*, 89 – 94.
[36] P. L. Hurst, J. Nielsen, P. A. Sullivan, M. G. Shepherd, *Biochem. J.* **1977**, *165*, 33 – 41.
[37] J. S. Luterbacher, L. P. Walker, J. M. Moran-Mirabal, *Biotechnol. Bioeng.* **2013**, *110*, 108 – 117.
[38] M. Santa-Maria, T. Jeoh, *Biomacromolecules* **2010**, *11*, 2000 – 2007.
[39] T. Imai, J. Sugiyama, *Macromolecules* **1998**, *31*, 6275 – 6279.
[40] T. Imai, J.-L. Putaux, J. Sugiyama, *Polymer* **2003**, *44*, 1871 – 1879.
[41] M. A. Jobst, C. Schoeler, K. Malinowska, M. A. Nash, *J. Vis. Exp.* **2013**, *82*, e50950.
[42] T. Abitbol, A. Palermo, J. M. Moran-Mirabal, E. D. Cranston, *Biomacromolecules* **2013**, *14*, 3278 – 3284.
[43] H. Gumpp, S. W. Stahl, M. Strackharn, E. M. Puchner, H. E. Gaub, *Rev. Sci. Instrum.* **2009**, *80*, 063704.

Received: May 16, 2014
Revised: June 12, 2014
Published online on August 12, 2014